Acoustic radiation of 2D nearly periodic metamaterial plates via finite element procedures and model reduction strategies

Jean-Mathieu Mencik, Marie-Laure Gobert

Acoustic radiation of 2D nearly periodic metamaterial plates via finite element procedures and model reduction strategies

J.-M. Mencik, M.-L. Gobert
INSA Centre Val de Loire, Université d'Orléans, Université de Tours,
Laboratoire de Mécanique Gabriel Lamé,
Rue de la Chocolaterie, 41000 Blois, France
e-mail: **jean-mathieu.mencik@insa-cvl.fr**

Abstract

The acoustic radiation of 2D nearly periodic plates interacting with light fluids is addressed. Metamaterial plates made up of resonant multi-layered cells/substructures with varying (random) geometrical properties, which are described via distorted finite element meshes, are dealt with. The proposed approach involves the Craig-Bampton method and an interpolation scheme for modeling the substructures and approximating the related reduced mass and stiffness matrices. In this paper, this approach is applied to compute the radiation efficiencies of such metamaterial plates with the method of elementary radiators. The relevance of the proposed approach is highlighted through numerical experiments. Especially the structural and acoustic responses of a nearly periodic plate are assessed and compared to the purely periodic case.

1 Introduction

In this paper, the acoustic radiation of 2D nearly periodic plates subjected to harmonic disturbance and interacting with light fluids (e.g., air) is addressed. 2D nearly periodic metamaterial plates made up of locally resonant cells – i.e., multi-layered substructures involving both soft and heavy materials which behave like multi-degree of freedom (DOF) mass-spring systems – are analyzed. For instance, a schematic of a nearly periodic plate with layered substructures (soft layer and heavy core), embedded in a floor panel and radiating in an acoustic fluid, is shown in Fig. 1. Here, the assumption is made that the substructures undergo geometrical changes which are introduced via distorted finite element (FE) meshes [1] as shown in Fig. 1. It is well known that purely periodic structures with resonant substructures possess band gap properties, i.e., frequency bands where waves do not propagate which, therefore, yield low vibration levels and low acoustic radiation. The question arises whether nearly periodic structures can provide additional features, e.g., the fact that the vibrational energy is localized to some parts of the structures [2, 3] which could bring additional benefits in the reduction of the sound levels.

To address the modeling of metamaterial plates made up of substructures with slightly varying random geometrical properties, the following approach can be used. The methodology is detailed in [1]. It involves moving the positions of the nodes of the FE mesh of a substructure using deterministic 2D shape functions (similar for each substructure) weighted by random variables (different between substructures). For computational purposes, reduced models of the substructures are considered. This implies computing their reduced mass and stiffness matrices via matrix interpolation, i.e., between a few interpolation points which represent some distorted configurations of the FE mesh. The modeling of a whole nearly periodic plate follows from FE assembly procedures. The proposed approach is intended to be general and can be used to model single or multiple plates, e.g., a nearly periodic plate embedded in a floor panel. Also, it can be straightforwardly used to model plates with spatially-varying mesh dispersion, e.g., purely periodic plates with localized nearly periodic regions.

Also, the present paper focuses on the acoustic radiation of 2D nearly periodic plates. Especially, the radiation efficiencies of baffled plates are assessed with the method of elementary radiators [4, 5]. For computational purposes, the radiation resistance matrices of the plates are approximated by considering a reduced spectral decomposition together with a linear frequency interpolation scheme. Numerical experiments are carried out on a 2D nearly periodic plate with 6×6 layered substructures. The advantages of nearly periodic plates against purely periodic ones for reducing the sound levels of structures are discussed.

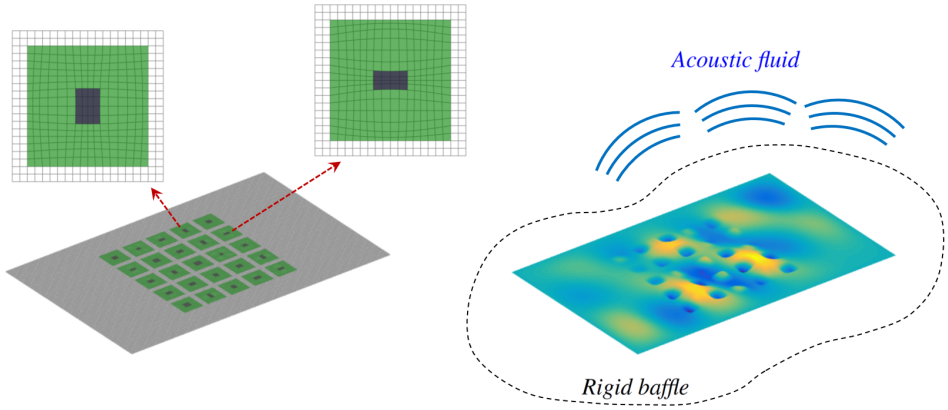

Figure 1: Radiating nearly periodic metamaterial plate embedded in a floor panel, and related transverse displacement field resulting from harmonic excitations.

2 Modeling of 2D nearly periodic plates

The methodology for modeling 2D nearly periodic structures is detailed in [1] and can be summarized as follows. Let us consider a nearly periodic plate made up of substructures with different (random) geometrical properties. The key idea here is to describe these substructures using distorted FE meshes (see Fig. 1), i.e., with node positions that randomly vary from a baseline/undistorted mesh. For a substructure s, this yields:

$$x_j^{se} = x_j^e + \epsilon_x^s f_x(x_j^e, y_j^e) \quad , \quad y_j^{se} = y_j^e + \epsilon_y^s f_y(x_j^e, y_j^e), \tag{1}$$

where (x_j^{se}, y_j^{se}) and (x_j^e, y_j^e) are the node coordinates of the distorted and undistorted meshes, respectively. Also, for each substructure s, ϵ_x^s and ϵ_y^s are two uniform random variables with support $[-\delta\,,\,\delta]$ (δ being a dispersion parameter). Finally, $f_x(x,y)$ and $f_y(x,y)$ are two arbitrary deterministic functions of (x,y), identical for all the substructures, which are supposed to vanish on the boundary.

The second step of the proposed approach is to consider reduced models of the substructures using the Craig-Bampton (CB) method. In this framework, the displacement vector of a substructure s with mass and stiffness matrices $\mathbf{M}^s$ and $\mathbf{K}^s$ is expressed in terms of static modes and fixed interface modes (a reduced number $M_{\mathtt{I}}$). The static modes represent the column vectors of the square matrix $-(\mathbf{K}^s_{\mathtt{II}})^{-1}\mathbf{K}^s_{\mathtt{IB}}$, where subscript $\mathtt{B}$ and subscript $\mathtt{I}$ denote boundary DOFs and internal DOFs, respectively. Also, the fixed interface modes represent the eigenvectors of the matrix pencil $(\mathbf{K}^s, \mathbf{M}^s)$ which are associated with its first $M_{\mathtt{I}}$ eigenvalues, and which represent the column vectors of the so-called reduced matrix $\widetilde{\mathbf{X}}^s$. By "projecting" the mass and stiffness matrices of each substructure s – namely, $\mathbf{M}^s$ and $\mathbf{K}^s$ – on the space spanned by the static modes and the fixed interface modes, the following reduced mass and stiffness matrices $\widetilde{\mathbf{M}}^s$ and $\widetilde{\mathbf{K}}^s$ can be obtained:

$$\widetilde{\mathbf{M}}^s = (\widetilde{\mathbf{T}}^s)^T \mathbf{M}^s \widetilde{\mathbf{T}}^s \quad , \quad \widetilde{\mathbf{K}}^s = (\widetilde{\mathbf{T}}^s)^T \mathbf{K}^s \widetilde{\mathbf{T}}^s \quad \text{where} \quad \widetilde{\mathbf{T}}^s = \begin{bmatrix} \mathbf{I} & \mathbf{0} \\ -(\mathbf{K}^s_{\mathtt{II}})^{-1}(\mathbf{K}^s_{\mathtt{IB}}) & \widetilde{\mathbf{X}}^s \end{bmatrix}. \tag{2}$$

Here, $\widetilde{\mathbf{T}}^s$ is the transformation matrix involved in the CB method. The modeling of a whole nearly periodic structure involving several substructures follows from classical FE assembly procedures.

This model reduction strategy, although well-known, is likely to suffer from high computational loading, however. Indeed, since the substructures are different – i.e., because of the fact that their geometrical properties randomly vary –, the transformation matrix $\widetilde{\mathbf{T}}^s$ (static and fixed interface modes) and the reduced matrices $\widetilde{\mathbf{M}}^s$ and $\widetilde{\mathbf{K}}^s$ (matrix projections) must be computed many times, i.e., as many times as the number of substructures considered. In this sense, the conventional CB method appears to be prohibitive. To address this issue, it is proposed to estimate the reduced matrices of the substructures via matrix interpolation. The idea is to compute these matrices at some points $\epsilon_x^s = (\epsilon_x)_p$ and $\epsilon_y^s = (\epsilon_y)_p$ (a small number) which represent some particular distorted FE meshes, and to estimate these matrices between these points via matrix interpolation, for any substructure and any mesh distortion parameters ϵ_x^s and ϵ_y^s.

To interpolate the reduced matrices of the substructures, they have to be expressed in compatible coordinate systems [6]. For that purpose, the following alternative reduced matrices of fixed interface modes can be considered at "interpolation points" $((\epsilon_x)_p, (\epsilon_y)_p)$ [1]:

$$\widehat{\mathbf{X}}_p = \widetilde{\mathbf{X}}_p (\boldsymbol{\Psi}^T \widetilde{\mathbf{X}}_p)^{-1}, \tag{3}$$

where

$$\boldsymbol{\Psi} = \left((\mathbf{M}_{\mathtt{II}}^0)^{\frac{1}{2}} \right)^T \widetilde{\mathbf{X}}^0. \tag{4}$$

Here, superscript 0 means that matrices are expressed at $\epsilon_x^s = 0$ and $\epsilon_y^s = 0$ (undistorted mesh); also, the matrix $\boldsymbol{\Psi}$ is supposed to be orthogonal. The criterion (3) means that the terms $\boldsymbol{\Psi}^T \widehat{\mathbf{X}}_p$ – i.e., the projections of the reduced matrices $\widehat{\mathbf{X}}_p$ on the column space of $\boldsymbol{\Psi}$ – are identical $\forall p$. Indeed, it can be verified that $\boldsymbol{\Psi}^T \widehat{\mathbf{X}}_p = \mathbf{I}$. In this framework, the following expressions for the transformation matrix and the reduced matrices at $\epsilon_x^s = (\epsilon_x)_p$ and $\epsilon_y^s = (\epsilon_y)_p$ can be proposed:

$$\widehat{\mathbf{T}}_p = \begin{bmatrix} \mathbf{I} & \mathbf{0} \\ -(\mathbf{K}_{\mathtt{II}})_p^{-1} (\mathbf{K}_{\mathtt{IB}})_p & \widehat{\mathbf{X}}_p \end{bmatrix} \quad , \quad \widehat{\mathbf{M}}_p = \widehat{\mathbf{T}}_p^T \mathbf{M}_p \widehat{\mathbf{T}}_p \quad , \quad \widehat{\mathbf{K}}_p = \widehat{\mathbf{T}}_p^T \mathbf{K}_p \widehat{\mathbf{T}}_p. \tag{5}$$

The determination of the reduced matrices for a substructure s with arbitrary mesh distortion parameters ϵ_x^s and ϵ_y^s follows from classic interpolation. For instance, an interpolation scheme based on eight interpolation points (ξ_p, η_p) and eight Serendipity interpolation functions $N_p(\xi^s, \eta^s)$ with parametric coordinates $\xi^s = \sqrt{2}\,\epsilon_x^s/\delta$ and $\eta^s = \sqrt{2}\,\epsilon_y^s/\delta$ can be considered as shown in Fig. 2 [1]. In this case, the reduced mass and stiffness matrices are obtained as follows:

$$\widehat{\mathbf{M}}^s = \sum_{p=1}^{8} N_p(\xi^s, \eta^s) \widehat{\mathbf{M}}_p \quad , \quad \widehat{\mathbf{K}}^s = \sum_{p=1}^{8} N_p(\xi^s, \eta^s) \widehat{\mathbf{K}}_p. \tag{6}$$

Reduced damping matrices of the substructures can be also considered. For instance, for Rayleigh type damping, the reduced damping matrices can be easily written as:

$$\widehat{\mathbf{C}}^s = a \widehat{\mathbf{M}}^s + b \widehat{\mathbf{K}}^s, \tag{7}$$

where a and b are damping coefficients. The modeling of a whole nearly periodic plate, based on the interpolated matrices $\widehat{\mathbf{M}}^s$, $\widehat{\mathbf{K}}^s$ and $\widehat{\mathbf{C}}^s$, follows from conventional FE procedures [1]. The related dynamic equilibrium equation, in the frequency domain (frequency $\omega/2\pi$), writes:

$$\left[-\omega^2 \widehat{\mathbf{M}}_{\mathtt{a}} + \mathtt{i}\omega \widehat{\mathbf{C}}_{\mathtt{a}} + \widehat{\mathbf{K}}_{\mathtt{a}} \right] \begin{bmatrix} (\widehat{\mathbf{u}}_{\mathtt{B}})_{\mathtt{a}} \\ \widehat{\boldsymbol{\alpha}}_{\mathtt{a}} \end{bmatrix} = \widehat{\mathbf{F}}_{\mathtt{a}}, \tag{8}$$

where $\widehat{\mathbf{M}}_{\mathtt{a}}$, $\widehat{\mathbf{K}}_{\mathtt{a}}$ and $\widehat{\mathbf{C}}_{\mathtt{a}}$ are the global mass, stiffness and damping matrices which are obtained by assembling the local matrices $\widehat{\mathbf{M}}^s$, $\widehat{\mathbf{K}}^s$ and $\widehat{\mathbf{C}}^s$ of the substructures; $(\widehat{\mathbf{u}}_{\mathtt{B}})_{\mathtt{a}}$ is the displacement vector for the boundary/interface nodes of the substructures; $\widehat{\boldsymbol{\alpha}}_{\mathtt{a}} = [(\widehat{\boldsymbol{\alpha}}^1)^T (\widehat{\boldsymbol{\alpha}}^2)^T \cdots]^T$ is the vector of generalized coordinates for the fixed interface modes of the substructures; $\widehat{\mathbf{F}}_{\mathtt{a}}$ is the vector of input forces. Also, in Eq. (8), $\mathtt{i}$ is the imaginary unit. To speed up the computation of the matrix equation (8), a model reduction consisting in

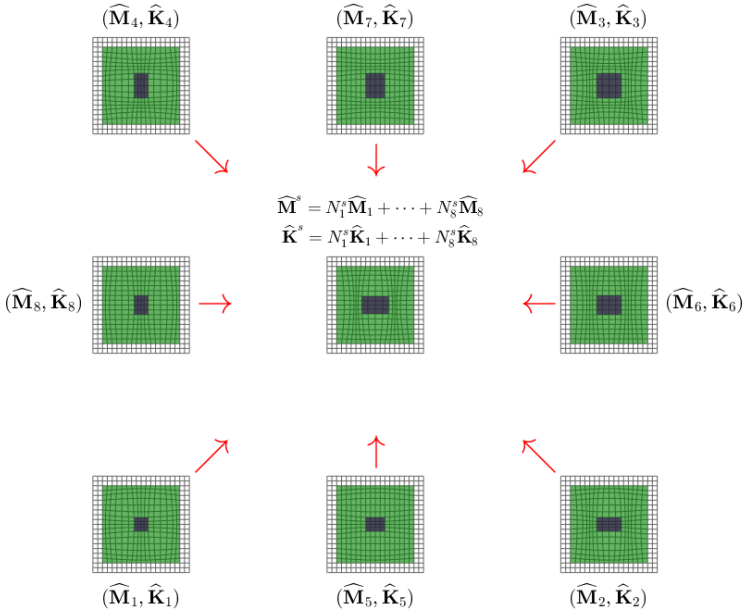

Figure 2: Eight point interpolation scheme based on Serendipity interpolation functions $N_p(\xi^s, \eta^s)$ $(p = 1, \ldots, 8)$.

describing the displacement vector $(\widehat{\mathbf{u}}_{\mathtt{B}})_{\mathtt{a}}$ with a reduced number of interface modes can be considered, i.e., $(\widehat{\mathbf{u}}_{\mathtt{B}})_{\mathtt{a}} = \widetilde{\mathbf{X}}^0_{\mathtt{a}}\widetilde{\boldsymbol{\beta}}_{\mathtt{a}}$ where $\widetilde{\mathbf{X}}^0_{\mathtt{a}}$ is a reduced matrix of interface modes. In order to avoid computing the interface modes for each change of the FE meshes of the substructures, those associated with the purely periodic plate (undistorted substructures) can be considered.

By solving Eq. (8), the displacement vector $(\widehat{\mathbf{u}}_{\mathtt{B}})_{\mathtt{a}}$ can be obtained and, therefore, the displacement vectors $\widehat{\mathbf{u}}^s_{\mathtt{B}}$ of the boundary nodes of the substructures. As for the displacement vectors $\widehat{\mathbf{u}}^s_{\mathtt{I}}$ of the internal nodes of the substructures, they can be easily obtained as:

$$\widehat{\mathbf{u}}^s_{\mathtt{I}} \approx -(\mathbf{K}^0_{\mathtt{II}})^{-1}\mathbf{K}^0_{\mathtt{IB}}\widehat{\mathbf{u}}^s_{\mathtt{B}} + \widehat{\mathbf{X}}^0\widehat{\boldsymbol{\alpha}}^s, \tag{9}$$

where $-(\mathbf{K}^0_{\mathtt{II}})^{-1}\mathbf{K}^0_{\mathtt{IB}}$ is the matrix of static modes when $\epsilon^s_x = 0$ and $\epsilon^s_y = 0$ (undistorted mesh), while matrix $\widehat{\mathbf{X}}^0$ is given by $\widehat{\mathbf{X}}^0 = \widetilde{\mathbf{X}}^0(\boldsymbol{\Psi}^T\widetilde{\mathbf{X}}^0)^{-1}$.

3 Acoustic radiation

The displacements of the substructures resulting from the approach proposed in Sec. 2 can be used to assess the acoustic radiation of a nearly periodic plate. In this framework, the vibrating plate is supposed to be surrounded by an infinite rigid baffle and immersed in a light acoustic fluid (e.g., air) where the fluid loading effects on the structure are neglected, see Fig. 1. Here, it is proposed to investigate the radiation efficiency σ of the plate, which is defined as the radiated sound power W_{rad} normalized by the product of the radiating surface area S_{plate} with the characteristic fluid impedance $\rho_0\, c_0$ and the space-averaged mean square normal velocity $< \mathbf{v}_n^2 >$ [7]:

$$\sigma = \frac{W_{rad}}{\rho_0\, c_0\, S_{plate}\, < \mathbf{v}_n^2 >}. \tag{10}$$

The radiation efficiency can be straightforwardly computed via the method of elementary radiators, see for instance [4, 5]. The strategy consists in modeling a vibrating plate as an assembly of N elementary radiators

j of elementary surfaces $S_{rad,j}$ and normal velocities $v_{n,j}$. In the frequency domain, this gives:

$$\sigma = \frac{\mathbf{v}_n^H \mathbf{R} \mathbf{v}_n}{\rho_0 \, c_0 \, S_{plate} < \mathbf{v}_n^2 >}, \tag{11}$$

where:

- $\mathbf{v}_n$ is the vector of normal velocities of the radiators, $\mathbf{v}_n = (v_{n,j})_{j=1,\ldots,N}$; under the light fluid assumption, $\mathbf{v}_n$ is directly linked to the vector of the *in vacuo* normal displacements $\mathbf{u}_n$ as:

$$\mathbf{v}_n = \mathtt{i}\omega \mathbf{u}_n; \tag{12}$$

- $\mathbf{R}$ is the resistance matrix whose components are expressed by:

$$R_{st} = \frac{\omega^2 \rho_0 \, S_{rad,s} \, S_{rad,t}}{4\pi c_0} \frac{\mathtt{sin}(k_0 \, r_{st})}{k_0 \, r_{st}} \quad (s \neq t) \quad , \quad R_{ss} = \frac{\omega^2 \rho_0 \, S_{rad,s}^2}{4\pi c_0}, \tag{13}$$

  where $k_0 = \omega / c_0$ is the acoustic wavenumber and r_{st} is the distance between the centers of two radiators s and t;

- $< \mathbf{v}_n^2 >$ is the mean square normal velocity averaged over the N elementary radiators:

$$< \mathbf{v}_n^2 > = \frac{1}{2} \frac{1}{N} \|\mathbf{v}_n\|^2. \tag{14}$$

Also, in Eq. (11), superscript H denotes the conjugate transpose.

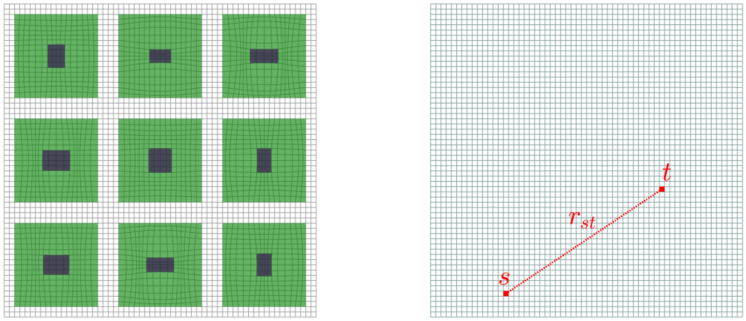

Figure 3: Distorted FE mesh (left) and distances r_{st} between two elementary radiators s and t used to compute the resistance matrix $\mathbf{R}$ (right).

Here, the elementary radiators are supposed to coincide with the elements of the FE mesh of the plate, i.e., the number of radiators N is equal to the number of elements of the FE mesh. For substructures with distorted FE meshes, the elementary surfaces $S_{rad,j}$ of the radiators are different and, therefore, they must be assessed element-wise from the positions of the nodes. Also, the normal displacements $u_{n,j}$ of the radiators can be obtained by averaging the normal displacements $(u_{n,j})_k$ at the nodes. These normal displacements can be obtained from the displacement vectors of the substructures, i.e., $\widehat{\mathbf{u}}_{\mathrm{B}}^s$ or $\widehat{\mathbf{u}}_{\mathrm{I}}^s$, see Sec. 2 and Eq. (9).

To avoid computing the resistance matrix $\mathbf{R}$ several times for substructures subject to geometrical changes (mesh distortion), the radiation efficiency is in practice computed as follows:

$$\sigma = \frac{\omega^2}{4\pi c_0^2 \, S_{plate} < \mathbf{v}_n^2 >} \mathbf{y}_n^H \mathbf{S} \, \mathbf{y}_n, \tag{15}$$

where $\mathbf{y}_n = (v_{n,j} \, S_{rad,j})_{j=1,\ldots,N}$ is the vector of normal velocities weighted by the radiator surfaces. Also, the matrix $\mathbf{S}$ is defined by:

$$S_{st} = \frac{\mathtt{sin}(k_0 \, r_{st})}{k_0 \, r_{st}} \quad (s \neq t) \quad , \quad S_{ss} = 1, \tag{16}$$

with r_{st} the distance between two radiator centers in the undistorted case, see Fig. 3; indeed it can be checked that the distance variations induced by the mesh distortion has a limited impact on the radiation levels, and that keeping the same distance values between the distorted and undistorted cases can help reduce the computational cost. Note that the resistance matrix $\mathbf{S}$ is fully-populated and depends on the wavenumber k_0, which also means that it depends on the frequency $\omega/2\pi$. As a result, the computation of the product $\mathbf{y}_n^H \mathbf{S} \mathbf{y}_n$ in Eq. (15) is prone to high computational loading. To solve this issue, a spectral decomposition of $\mathbf{S}$ can be invoked [4, 7]. First note that the matrix $\mathbf{S}$ is real, symmetric and positive definite. Then, it admits the following spectral decomposition $\mathbf{S} = \boldsymbol{\Phi}\boldsymbol{\Lambda}\boldsymbol{\Phi}^T = \boldsymbol{\Phi}\boldsymbol{\Lambda}\boldsymbol{\Phi}^H$ where $\boldsymbol{\Lambda} = \mathtt{diag}\{\lambda_k\}_{k=1}^N$ and $\boldsymbol{\Phi} = [\boldsymbol{\phi}_1 \cdots \boldsymbol{\phi}_N]$ are the related matrices ($N \times N$) of eigenvalues λ_k and eigenvectors $\boldsymbol{\phi}_k$ (respectively). By retaining a reduced number $M \ll N$ of largest eigenvalues $\{\lambda_1, \ldots, \lambda_M\}$, the following reduced spectral decomposition can be proposed, $\mathbf{S} \approx \widetilde{\boldsymbol{\Phi}}\widetilde{\boldsymbol{\Lambda}}\widetilde{\boldsymbol{\Phi}}^H$ where $\widetilde{\boldsymbol{\Lambda}} = \mathtt{diag}\{\lambda_k\}_{k=1}^M$ ($M \times M$ matrix) and $\widetilde{\boldsymbol{\Phi}} = [\boldsymbol{\phi}_1 \cdots \boldsymbol{\phi}_M]$ ($N \times M$ matrix). In this case, the product $\mathbf{y}_n^H \mathbf{S} \mathbf{y}_n$ in Eq. (15) simplifies to:

$$\mathbf{y}_n^H \mathbf{S} \mathbf{y}_n \approx \widetilde{\mathbf{y}}_n^H \widetilde{\boldsymbol{\Lambda}} \widetilde{\mathbf{y}}_n = \sum_{j=1}^{M} \lambda_j |\widetilde{y}_{n,j}|^2, \tag{17}$$

where:

$$\widetilde{\mathbf{y}}_n = \widetilde{\boldsymbol{\Phi}}^H \mathbf{y}_n. \tag{18}$$

While efficient, the above strategy does not solve the issue of computing the matrix $\mathbf{S}$ at each frequency. This constitutes the most expensive numerical task, especially when the number of elementary radiators N is high. To address this issue, an interpolation strategy can be considered in the frequency domain. In this framework, it is proposed to compute the reduced matrices $\widetilde{\boldsymbol{\Lambda}}$ and $\widetilde{\boldsymbol{\Phi}}$ at some master frequencies $\Omega_1/2\pi, \ldots, \Omega_P/2\pi$, and interpolate these matrices between two consecutive interpolation points $\Omega_k/2\pi$ and $\Omega_{k+1}/2\pi$ ($k = 1, \ldots, P-1$) via linear interpolation, i.e.:

$$\widetilde{\boldsymbol{\Lambda}}(\omega) = \frac{\Omega_{k+1} - \omega}{\Omega_{k+1} - \Omega_k} \widetilde{\boldsymbol{\Lambda}}_k + \frac{\omega - \Omega_k}{\Omega_{k+1} - \Omega_k} \widetilde{\boldsymbol{\Lambda}}_{k+1}, \qquad \Omega_k \leq \omega \leq \Omega_{k+1}, \qquad k = 1, \ldots, P-1 \tag{19}$$

$$\widetilde{\boldsymbol{\Phi}}(\omega) = \frac{\Omega_{k+1} - \omega}{\Omega_{k+1} - \Omega_k} \widetilde{\boldsymbol{\Phi}}_k + \frac{\omega - \Omega_k}{\Omega_{k+1} - \Omega_k} \widetilde{\boldsymbol{\Phi}}_{k+1}, \qquad \Omega_k \leq \omega \leq \Omega_{k+1}, \qquad k = 1, \ldots, P-1. \tag{20}$$

To ensure the applicability of the interpolation strategy, the column vectors of two reduced matrices $\widetilde{\boldsymbol{\Phi}}_k$ and $\widetilde{\boldsymbol{\Phi}}_{k+1}$ between two consecutive master frequencies $\Omega_k/2\pi$ and $\Omega_{k+1}/2\pi$ must be ordered in the same way. This may not be verified, for instance, in case of double eigenvalues. The use of a MAC criterion [8, 9] can help fix this issue. In this framework, a temporary reduced matrix $\widetilde{\boldsymbol{\Phi}}'_{k+1} = [\boldsymbol{\phi}'_1, \ldots, \boldsymbol{\phi}'_M]_{k+1}$ is computed at the master frequency $\Omega_{k+1}/2\pi$, and the following $M \times M$ MAC matrix is considered:

$$\mathtt{MAC}(i,j) = \frac{|(\boldsymbol{\phi}_i)_k^T (\boldsymbol{\phi}'_j)_{k+1}|^2}{\|(\boldsymbol{\phi}_i)_k\|^2 \, \|(\boldsymbol{\phi}'_j)_{k+1}\|^2}. \tag{21}$$

The M eigenvectors $(\boldsymbol{\phi}'_j)_{k+1}$ are then sorted in $\widetilde{\boldsymbol{\Phi}}_{k+1}$ in an iterative way according to the largest MAC values. The eigenvalues are sorted accordingly in the matrix $\widetilde{\boldsymbol{\Lambda}}_{k+1}$.

4 Numerical results

The proposed approach is validated through numerical experiments. Here, a simply supported nearly periodic plate with 6×6 substructures subjected to a point harmonic force and surrounded by a rigid baffle is considered as shown in Fig. 4. Typical distorted substructures are shown in Fig. 1 and are meshed using 20×20 isoparametric quadratic Mindlin elements. Square substructures with dimensions 0.25×0.25 m^2 are considered which involve a core in tungsten (density of 19250 kg/m^3, Young's modulus of 340 GPa, Poisson's ratio of 0.27), a medium layer in rubber (density of 950 kg/m^3, Young's modulus of 0.15 GPa, Poisson's ratio of 0.48) and an external layer in steel (density of 7850 kg/m^3, Young's modulus of 220 GPa,

Poisson's ratio of 0.3). Hence, the substructures are built from soft and stiff/heavy materials and, as such, exhibit a resonant behavior. Concerning the distorted meshes of the substructures, trigonometric "shape" functions $f_x(x_j^e, y_j^e)$ and $f_y(x_j^e, y_j^e)$ with a dispersion parameter $\delta = 0.01$ m are used, see Eq. (1).

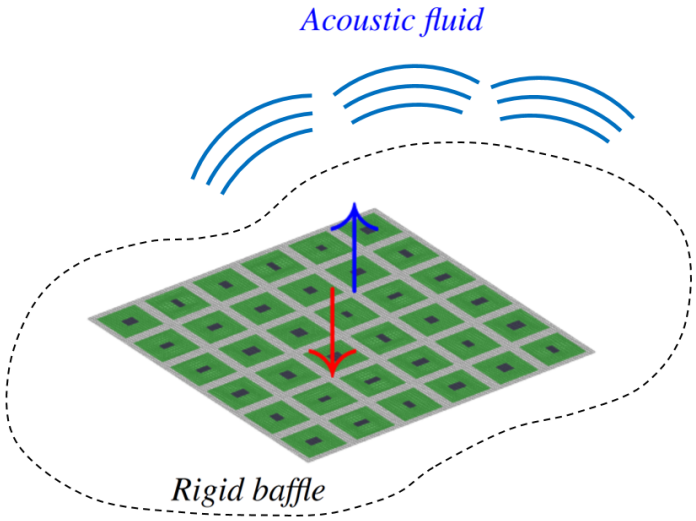

Figure 4: Schematic of a nearly periodic plate with 6×6 substructures vibrating in an acoustic fluid: (red arrow) input harmonic force; (blue arrow) measurement point.

First, the dynamic analysis of the nearly periodic plate vibrating *in vacuo* is carried out, see Sec. 2. The frequency responses of the structure – i.e., the quadratic velocity at some measurement point (see Fig. 4) – resulting from the interpolation strategy and the classical FE method are shown in Fig. 5 over a frequency band of $[0.1\ ,\ 150]$ Hz (frequency resolution $\Delta f = 0.1$ Hz). Concerning the interpolation strategy and the related CB method, $M_{\mathrm{I}} = 5$ fixed interface modes are used to model the substructures. The strategy for determining M_{I} consists in selecting the modes whose eigenfrequencies are below two or three times the maximum frequency of the frequency band analyzed (150 Hz here). The reduced mass and stiffness matrices follow from Eqs. (5) and (6). Also, the reduced damping matrices follow from Eq. (7) with $a = 5 \times 10^{-3}$ s^{-1} and $b = 2 \times 10^{-6}$ s.

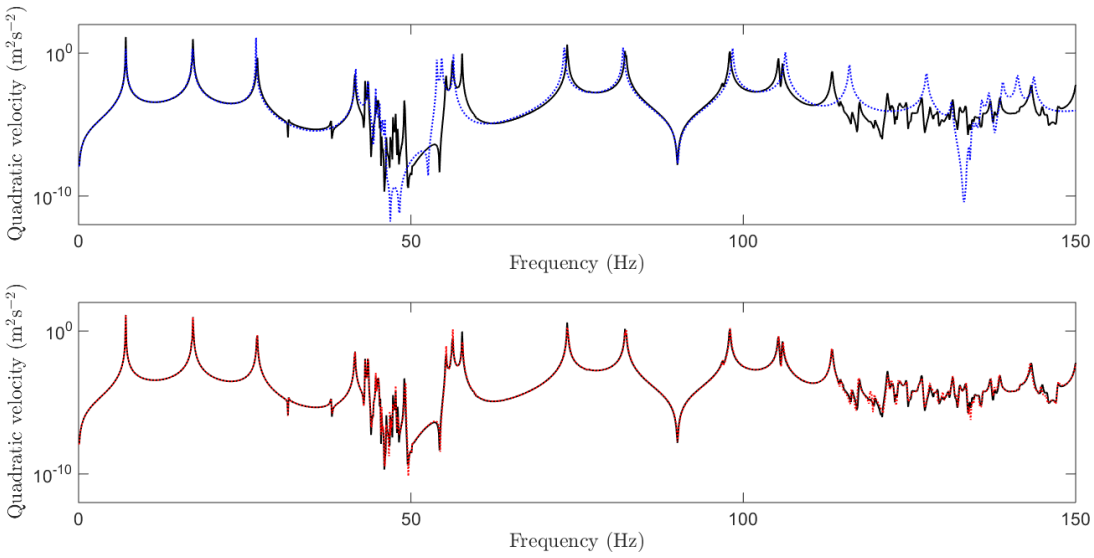

Figure 5: Frequency responses (quadratic velocity): (black solid line) FE method, nearly periodic plate; (red dotted line) interpolation strategy, nearly periodic plate; (blue dotted line) FE method, purely periodic plate.

Within the framework of the proposed approach, the displacement solution is obtained by solving Eq. (8). To reduce the computational burden associated with the resolution of this equation, a model reduction based on 400 interface modes (matrix $\widetilde{\mathbf{X}}_{\mathrm{a}}^{0}$) is considered as discussed earlier, see comments after Eq. (8). As it can be seen in Fig. 5, the frequency response of the nearly periodic plate issued from the interpolation strategy closely matches the reference FE solution. This, therefore, validates the proposed approach. For comparison purposes, the harmonic response of the purely periodic plate is also shown. It is observed that the purely periodic and nearly periodic solutions are different. The key results here are: (i) in the purely periodic case, the harmonic response is characterized by localized frequency bands with low vibration levels, around 45 Hz and 135 Hz (band gaps); (ii) overall the vibration levels of the nearly periodic plate at high frequencies (after 100 Hz) are small compared to the purely periodic case.

Also, the radiation efficiencies of the purely periodic and nearly periodic plates are computed from Eq. (15), where the plates are supposed to radiate in air (density $\rho_0 = 1$ kg/m^3, wave speed $c_0 = 330$ m/s). The number of elementary radiators is equal to the number of elements of the FE meshes of the plates (as explained earlier), that is $N = 14,400$. For both the purely periodic and nearly periodic cases, reference FE solutions are considered. These are obtained by computing the vectors of normal displacements $\mathbf{u}_n$ of the plates at each frequency (frequency band of $[0.1\,,\,150]$ Hz, frequency step $\Delta f = 0.1$ Hz) by solving the full FE models of the structures. The resulting radiation efficiencies (reference solutions) are displayed in Fig. 6.

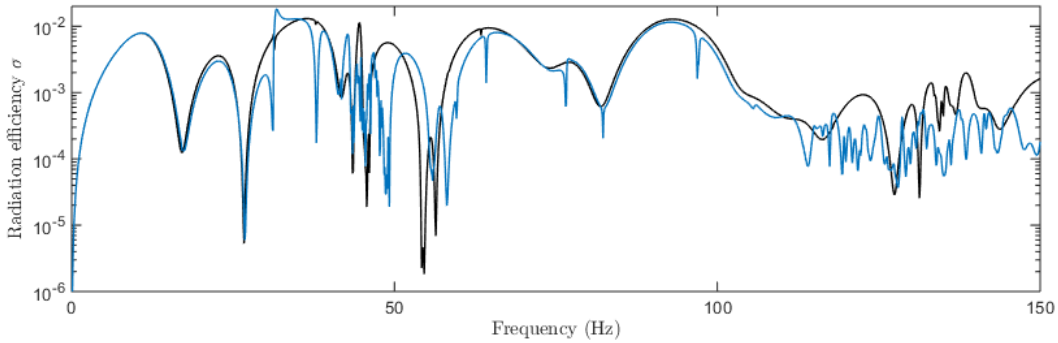

Figure 6: Radiation efficiencies obtained with the FE method: (black solid line) purely periodic plate; (blue solid line) nearly periodic plate.

In Fig. 6, it is shown that the acoustic radiation of the plate is affected by the mesh distortion. Overall the acoustic levels of the purely periodic and nearly periodic plates are of the same order of magnitude up to 100 Hz despite some local decreases of the nearly periodic solution. However, the acoustic levels appear to be globally low and smooth after 100 Hz in benefit of the nearly periodic case, the resonance effects being less pronounced. These results open interesting prospects in the acoustic control of mechanical systems which would deserve to be better explored, however.

Also, the radiation efficiencies of the plates can be computed via the proposed approach, see Sec. 2 and Sec. 3. To this end, $M = 12$ (among $14,400$) eigenvalues and eigenvectors are retained in the spectral decomposition of the matrix $\mathbf{S}$. The retained eigenvalues and eigenvectors are computed at $P = 16$ master frequencies $\Omega_k/2\pi$ equally spaced within $[0.1\,,\,150]$ Hz, i.e., with a frequency step $\Delta f' \approx 10$ Hz which is about one hundred times bigger than the original frequency step $\Delta f = 0.1$ Hz. Recall that, between two consecutive master frequencies, the resistance matrix $\mathbf{S}$ is estimated via linear interpolation, see Eqs. (19) and (20). The approximated radiation efficiencies are shown in Fig. 7 along with the reference FE solutions. For both the purely periodic and nearly periodic cases, the proposed solutions are in good agreement with the reference ones. Concerning the nearly periodic case, small discrepancies occur after 100 Hz, which however do not alter the overall vibroacoustic behavior and the sound attenuation effects reported earlier. Concerning computational saving, the time reduction for computing the acoustic radiation efficiencies with the proposed approach is about 95% when compared to the classical FE method. This offers the possibility to carry out more systematic studies, e.g., to optimize the acoustic radiation attenuation of nearly periodic structures.

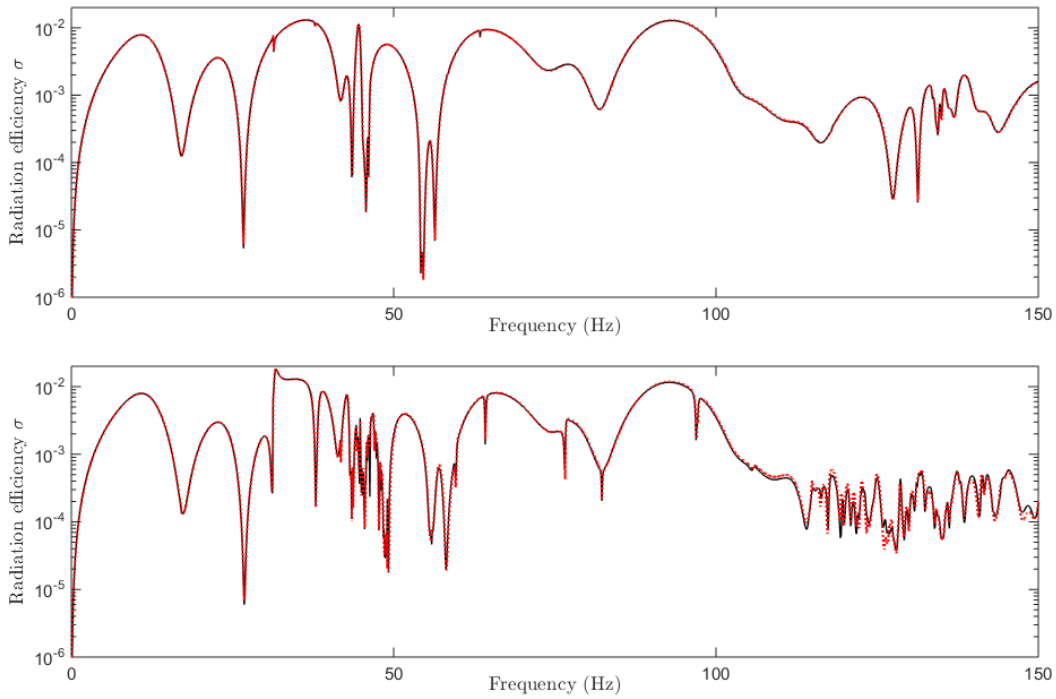

Figure 7: Radiation efficiencies obtained with the FE method (black solid line) and the proposed approach (red dotted line): (top) purely periodic plate; (bottom) nearly periodic plate.

5 Conclusion

The acoustic radiation of 2D nearly periodic metamaterial plates made up of resonant substructures with distorted FE meshes has been addressed via reduced models. The proposed approach enables fast computation of the frequency responses of the structures. This involves expressing the reduced matrices of the substructures via matrix interpolation. The resulting structural displacements can be post-processed to compute the radiation efficiencies of nearly periodic plates via the method of elementary radiators. To alleviate the computational burden for determining the radiation efficiencies at many frequencies, a reduced spectral decomposition of the resistance matrix together with a linear frequency interpolation scheme for the retained eigenvalues and eigenvectors are considered. The resulting vibroacoustic solutions can be efficiently computed and are in good agreement with the reference ones. Compared to the purely periodic case, nearly periodic plates yield overall reduced sound levels at high frequencies which appears promising in the acoustic control of mechanical systems.

References

[1] J.-M. Mencik, “Model reduction based on matrix interpolation and distorted finite element meshes for dynamic analysis of 2D nearly periodic structures,” *Finite Elements in Analysis and Design*, vol. 188, p. 103518, 2021.

[2] M. Castanier and C. Pierre, “Individual and interactive mechanisms for localization and dissipation in a mono-coupled nearly-periodic structure,” *Journal of Sound and Vibration*, vol. 168, no. 3, pp. 479–505, 1993.

[3] F.-M. Li and Y.-S. Wang, “Study on wave localization in disordered periodic layered piezoelectric composite structures,” *International Journal of Solids and Structures*, vol. 42, pp. 6457–6474, 2005.

[4] S. J. Elliott and M. E. Johnson, "Radiation modes and the active control of sound power," *Journal of the Acoustical Society of America*, vol. 94, no. 4, pp. 2194–2204, 1993.

[5] J.-M. Mencik and M.-L. Gobert, "Wave finite element based strategies for computing the acoustic radiation of stiffened or non-stiffened rectangular plates subject to arbitrary boundary conditions," *Proceedings of the 11th International Conference on Computational Structures Technology (CST 2012), Dubrovnik, Croatia*, pp. 3272–3291, 2012.

[6] H. Panzer, J. Mohring, R. Eid, and B. Lohmann, "Parametric model order reduction by matrix interpolation," *at-Automatisierungstechnik*, vol. 58, no. 8, pp. 475–484, 2010.

[7] J. Arenas and M. Crocker, "Sound radiation efficiency of a baffled rectangular plate excited by harmonic point forces using its surface resistance matrix," *International Journal of Acoustics and Vibration*, vol. 7, no. 4, pp. 217–22, 2002.

[8] M. Pastor, M. Binda, and T. Harcarik, "Modal assurance criterion," *Procedia Engineering*, vol. 48, pp. 543–548, 2012.

[9] J.-M. Mencik and M. N. Ichchou, "Multi-mode propagation and diffusion in structures through finite elements," *European Journal of Mechanics - A/Solids*, vol. 24, no. 5, pp. 877–898, 2005.